Int. J. Electrochem. Sci., 1(**2006**)110-121

International Journal of ELECTROCHEMICAL SCIENCE
www.electrochemsci.org

A New Type of Lithium-ion Battery Based on Tin Electroplated Negative Electrodes

J. Hassoun, S. Panero, P. Reale and B. Scrosati

Department of Chemistry, University of Rome "La Sapienza", 00185 Rome, Italy
*E-mail: bruno.scrosati@uniroma1.it

Received: 29 May 2006 / *Accepted:* 14 June 2006 / *Published:* 16 June 2006

This work describes the preparation and the characterization of various samples of metallic Sn electroplated on a cupper foil under different current and time regimes. These samples have been characterized by XRD and SEM and tested as negative electrodes in a cell using lithium foil as the counter electrode. The best electrode has been cycled with a capacity in the order of 990 $mAhg^{-1}$, i.e. approaching 100 % of theoretical capacity at 1 equivalent Li alloying. This electrode was also tested under a limited capacity regime (400 $mAhg^{-1}$) showing an interesting cycle life. Finally, the electrode was used as anode in a lithium-ion cell with $LiNi_{0.5}Mn_{1.5}O_4$ as cathode. This cell performed well at high rate (1C rate), delivering high capacity and excellent charge-discharge efficiency for a limited amount of cycles.

Keywords: lithium ion battery, Sn electrode, discharge capacity

1. INTRODUCTION

Lithium-tin alloys have high specific capacity and they are considered as promising negatives electrodes in lithium-ion batteries in replacement of carbon based materials [1-5]. The main issue of these alloys is the large volume expansion-contraction experienced during the charge-discharge cycling process which induces mechanical disintegration, this finally resulting in a very poor cycle life. A way to solve this problem is to cycle the electrode under limited capacity. This reduces the fraction of lithium inserted in the tin lattice and accordingly, controls the volume variation.

Ball milling [4,5[, sol-gel precipitation [6] and electroplating [1,3,7,8] are possible routes for the synthesis of tin based compounds or tin-carbon mixtures. The easiest and most controllable technique for obtaining thin, morphological optimized and electrochemical active films is the electrodeposition [8].

In this work we have investigated the conditions and the parameters for the electrodeposition of tin negative electrodes with the aim of optimizing their use as effective negative electrodes in lithium ion batteries.

2. EXPERIMENTAL PART

Tin samples were obtained by electroplating on a copper foil in a two-electrode glass cell. An aqueous solution, formed by KCl 0.15M, $SnCl_2$ 0.175M, $K_4P_2O_7$ 0.5M, glycine 0.125 M and NH_4OH 5ml/l, was used as the electrolyte [7] and a Pt foil as the counter electrode. The electroplating current and time conditions were monitored using a Maccor Series 4000 Battery Test System.

The structure of the samples was controlled by XRD, using a Rigaku X-ray diffractometer miniflex and their morphology by Scanning Electron Microscopy, SEM, using SEM Leo EVO 40.

The electrochemical response of the samples was tested in a cell based on the following sequence: i) a working electrode formed by the given Sn sample electrodeposited on a copper foil (which acted as current collector), ii) a 1M $LiPF_6$ in ethylene carbonate-dimethyl carbonate, EC:DMC 1:1 (Merck Battery Grade) electrolyte solution soaked on a Whatman™ separator and iii) a lithium metal foil counter electrode. The cell was cycled at 0.8C (around 1 $Acm^{-2}g^{-1}$ vs. Sn active mass) and within a 0,02-1,5 V voltage limit, using a Maccor Series 4000 Battery Test System as the controlling instrument. For the limited capacity test the cell was cycled at 0,2 mAh (400 $mAhg^{-1}$ vs. Sn Active mass).

The lithium-ion cell was formed by coupling the selected Sn sample anode with a $LiNi_{0.5}Mn_{1.5}O_4$ cathode [9] in a 1M $LiPF_6$ EC:DMC 1:1 electrolyte solution. Lithium foil was also added as counter electrode for anode and cathode activation. The cathode was prepared as a thin film on an aluminium substrate by doctor-blade deposition of a slurry composed of 80% $LiNi_{0.5}Mn_{1.5}O_4$ (active material), 10% PVdF 6020, Solvay Solef (binder) and 10% SP carbon (electronic support). Prior to cell testing, the $LiNi_{0.5}Mn_{1.5}O_4$ cathode was activated by charging versus lithium from open circuit voltage (OCV) to 5 V at C/5 rate (around 40 $mAcm^{-2}g^{-1}$) and the Sn anode by discharging versus lithium from OCV to 0.01 V at C/24 rate (around 53 $mAcm^{-2}g^{-1}$). The cell was then cycled at 1C (around 0.2 $Acm^{-2}g^{-1}$vs. cathode) and within a 3.0-5.0 V voltage limit, using a Maccor Series 4000 Battery Test System as the controlling instrument. The cell was limited by cathode at the theoretical capacity of 0.2 mAh (147.8 $mAhg^{-1}$) which correspond at 400 $mAhg^{-1}$ considering Sn active mass.

3. RESULTS AND DISCUSSION

In order to investigate the role of the synthesis conditions in affecting the electrochemical properties of the final products, we have prepared six Sn samples electrodeposited under different current and time regimes, keeping the charge at the value of 1.8 coulomb cm^{-2}. The preparation conditions of these samples are summarized in Table 1.

Table 1. Electroplating parameters of the Sn samples investigated in this work.

Sample	Electrodeposition current, $mAcm^{-2}$	Electrodeposition time, minutes
Sn-1	0.5	60
Sn-2	1.0	30
Sn-3	2.0	15
Sn-4	3.0	10
Sn-5	6.0	5
Sn-6	15	2

First, XRD was used to check the structural characteristics of the six samples. Figure 1 shows the evolution of the diffraction spectra passing from sample Sn-1 to sample Sn-6. As expected, the peaks of all samples can be ascribed to the Sn phase. The crystallinity of the samples remains constant passing from sample Sn-1 to sample Sn-5 and it decreases moving to sample Sn-6. The structural evolution seems to be related to the kinetics of the electrodeposition process, which in turn is affected by the synthesis conditions which include the change of current density magnitude order passing from samples Sn-1, 5 to Sn-6, time and so on.

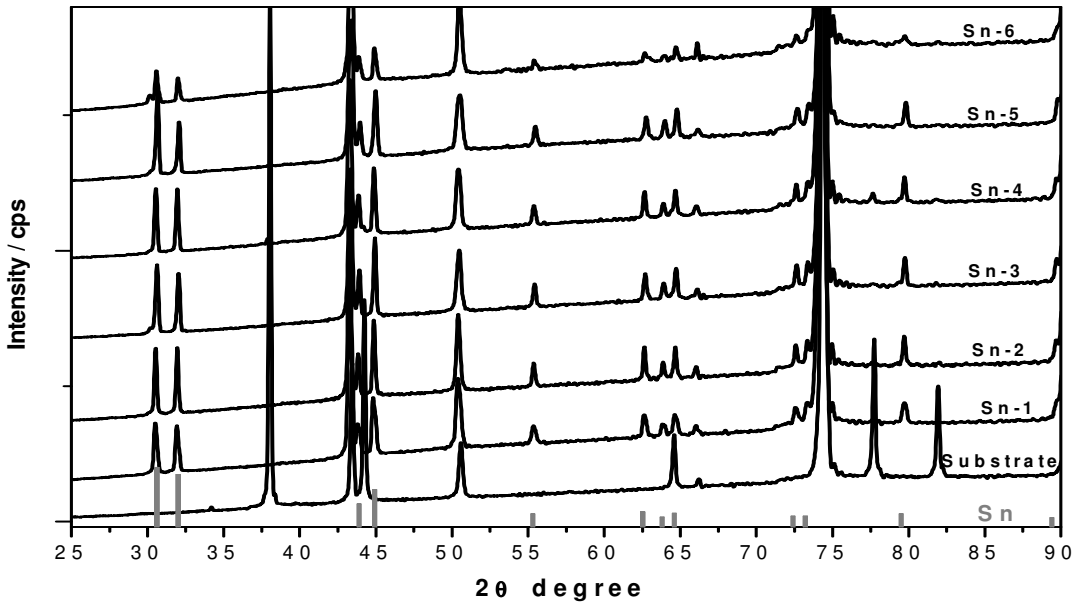

Figure 1. XRD patterns of the various Sn samples prepared by electroplating on a Cu foil at different current density/time regimes. For samples' identification see Table 1.

Figures 2 A-F, show in comparison the morphology of the various electrodeposited samples as evaluated by SEM investigation. Substantial differences among the samples can be observed. Samples Sn-1, Sn-2, Sn-3 and Sn-4 have a thread form morphology, see figures 2A,B,C,D. This morphology progressively changes for the samples electrodeposited at increasing current values. Accordingly sample Sn-5 has a porous pillars morphology, figure 2E, and sample Sn-6 has an extended, granular porosity characterized by small pillars, Figure 2F.

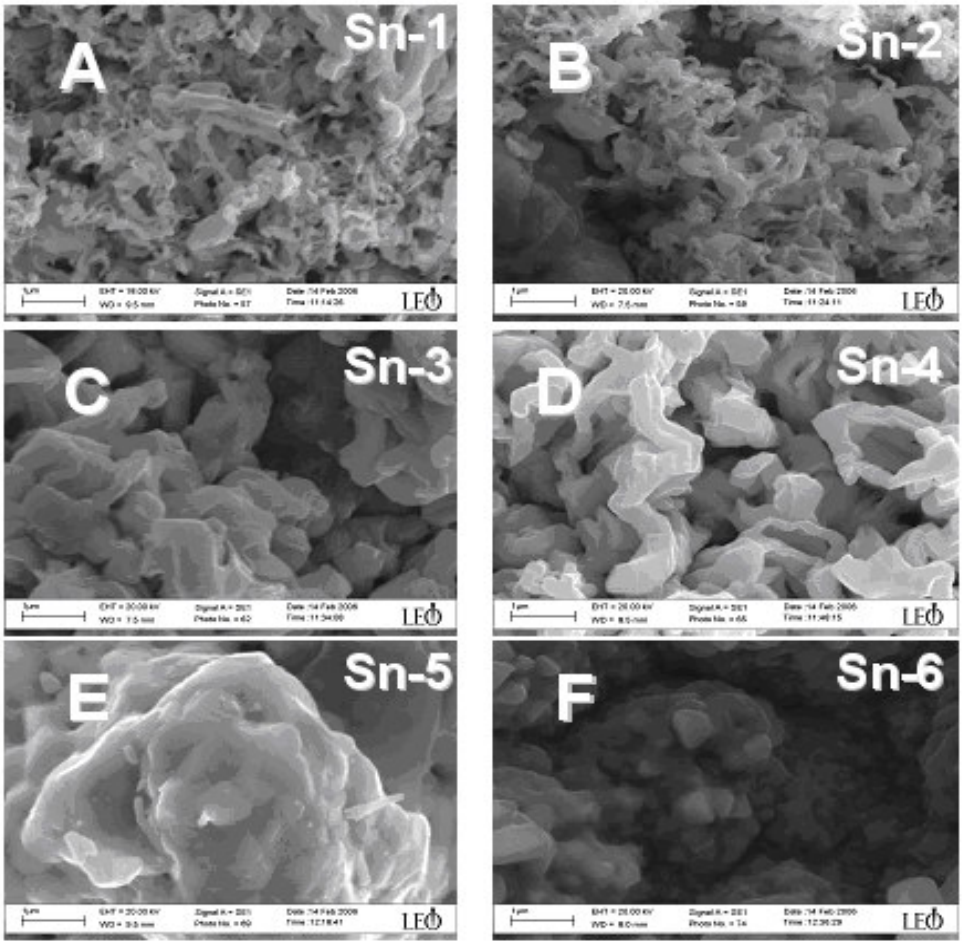

Figure 2 SEM images of the various Sn samples investigated in this work: Sn-1 (A); Sn-2 (B); Sn-3 (C); Sn-4 (D); Sn-5 (E); Sn-6 (F). For samples' identification see Table 1.

These differences in morphology are expected to reflect in differences in the electrochemical behaviour. This has been verified by examining the cycling response of the various samples in a lithium cell. It is assumed that the electrochemical process of this cell is the following:

Discharge: $Sn + 4.4Li^+ + 4.4\ e^- \Rightarrow Li_{4.4}Sn$ (1)

Charge: $Li_{4.4}Sn \Rightarrow Sn + 4.4Li^+ + 4.4\ e^-$ (2)

Process (1) suggest that, under steady-state electrochemical operation, the tin electrode has a total theoretical capacity of 993 $mAhg^{-1}$.

Figure 3 shows the capacity delivered upon discharge (see process (1)) when cycling of samples Sn-1, Sn-2, Sn-3, Sn-4, Sn-5, and Sn-6, respectively, when cycled versus a lithium foil counter electrode. Figure 4 illustrates the respective voltage profiles at the 9th cycle.

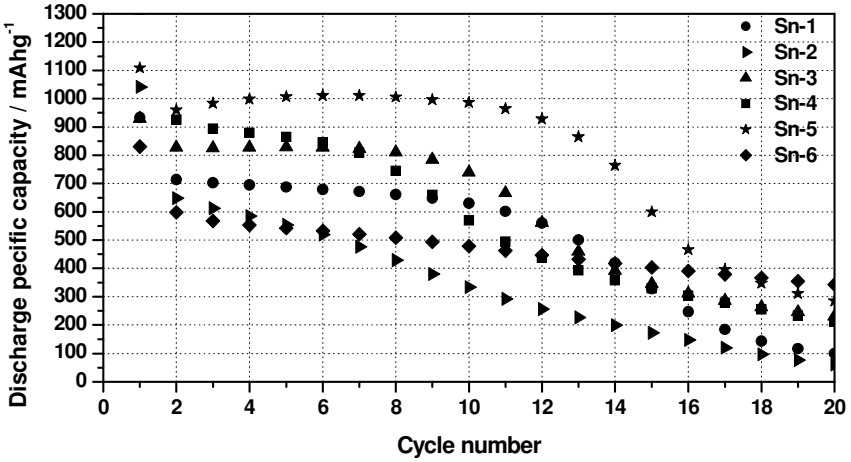

Figure 3. Discharge capacity delivered upon cycling of lithium cells using samples Sn-1, Sn-2, Sn-3, Sn-4, Sn-5, and Sn-6, respectively, as cathode. EC:DMC 1:1 $LiPF_6$ electrolyte. Charge-discharge current density: 1Acm^{-2}g^{-1}, about 0.8C rate.Room temperature. For samples' identification see Table 1.

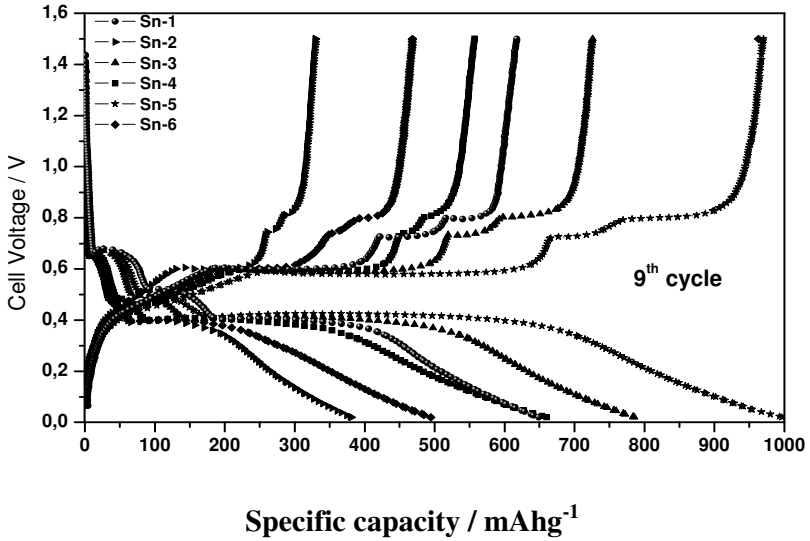

Figure 4. Voltage profiles at the 9th cycle of lithium cells using samples Sn-1, Sn-2, Sn-3, Sn-4, Sn-5, and Sn-6, respectively, as cathodes. EC:DMC 1:1 LiPF6 electrolyte. Charge-discharge current density: 1Acm-2g-1, about 0.8C rate. Room temperature. For samples' identification see Table 1.

Examining Figure 3 we observe an initial decay in capacity when passing from the first to the following cycles. Probably, this is associated to the formation of an passivation film on the electrode surface. The decay in capacity vanishes in the following cycles which evolve with a high charge-discharge efficiency, see Figure 4. In this steady-state regime, the cells operate in charge and in discharge according to processes (2) and (1), respectively, which are reversible.

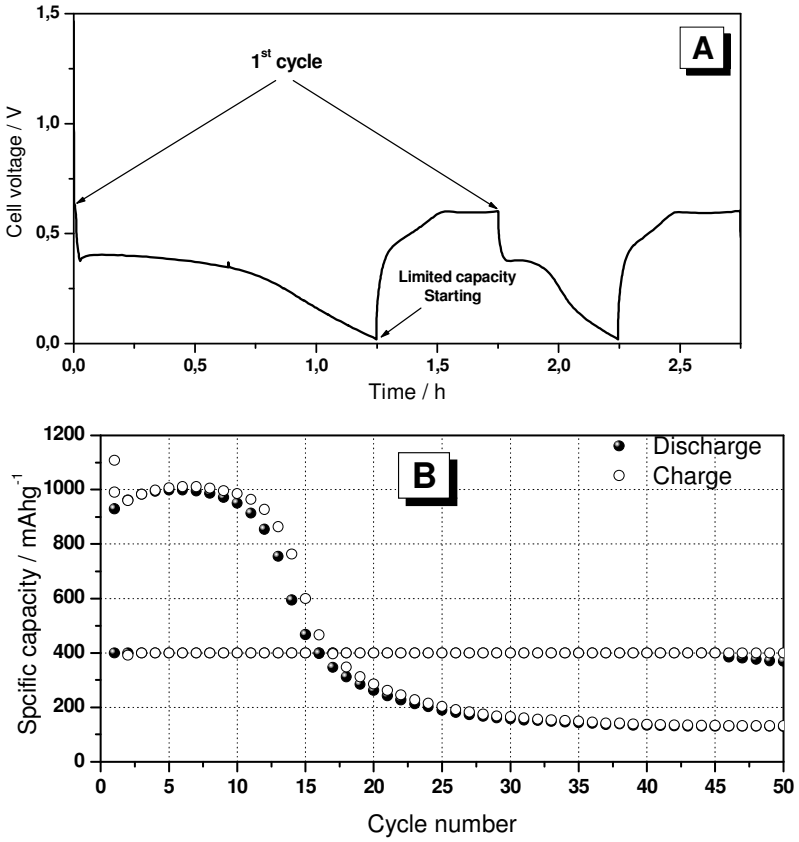

Figure 5. Cell voltage vs. time profiles for 1st and 2nd cycle for limited capacity test and comparison between specific capacity vs. cycle number profiles for limited capacity and full capacity tests using sample Sn-5 as cathode in a lithium cell, EC:DMC 1:1 $LiPF_6$ electrolyte. Charge-discharge current density: $1Acm^{-2}g^{-1}$, about 0.8C rate. Room temperature. For samples' identification see Table 1.

All samples deliver high specific capacity; however, the cycle life is poor. The best performance is offered by cells based on sample "Sn-5" having a porous pillars morphology, see Fig. 2E. Under steady-state regime, this sample delivers up to 990 $mAhg^{-1}$, a values which approaches 100 % of the theoretical capacity expected by process (1). These is an impressive performance, especially considering the high rate at which the cycles are run, i.e 0.8C. Cells based on the other samples have lower delivered capacity and comparably poor cycle life.

Indeed, a poor cycle life is expected for this type of electrodes, which are affected by large volume variations upon lithium uptake-release. A valid approach for improving the life is to cycle the electrode at a controlled, limited capacity regime, in order to reduce the fraction of lithium inserted in tin lattice and thus, reduce the extent of the volume variation.

Figure 5A shows a typical voltage vs. time profiles of a capacity-limited test for sample Sn-5 versus a lithium foil counter electrode. The first discharge is run at full capacity while the following charge-discharge cycles are run at a limited capacity of 0.2 mAh (400 $mAhg^{-1}$ versus tin active mass).

Figure 5B, which compares the response under these controlled capacity conditions with that related to full capacity cycling, clearly evidences the improvement obtained both in life (extending to 50 cycle) and to charge-discharge efficiency (approaching 100 %).

Figure 6 shows cell voltage vs. specific capacity profiles for 1^{st} and 10^{th} , 20^{th} , 30^{th} , 40^{th} and 50^{th} cycle for limited capacity test. In the 1^{st} cycle, Figure 6A, we see only the profile related to first tree steps described by processes (3), (4), (5) which characterized the Li-Sn alloying mechanism (10):

- $5Sn + 2Li + 2e^- \leftrightarrows Li_2Sn_5$ (3)
- $Li_2Sn_5 + 3Li + 3e^- \leftrightarrows 5LiSn$ (4)
- $3LiSn + 4Li + 4e^- \leftrightarrows Li_7Sn_3$ (5)
- $2Li_7Sn_3 + Li + e^- \leftrightarrows 3Li_5Sn_2$ (6)
- $5Li_5Sn_2 + Li + e^- \leftrightarrows 2Li_{13}Sn_5$ (7)
- $2Li_{13}Sn_5 + 9Li + 9e^- \leftrightarrows 5Li_7Sn_2$ (8)
- $5Li_7Sn_2 + 9Li + 9e^- \leftrightarrows 2Li_{22}Sn_5$ (9)

Progressively, this profile changes and becomes representative of all the steps of Li-Sn alloying process, i.e. steps (3) to (9), see figures 6B to 6F. A tentative explanation is to assume, as the cycling proceeds, the extent of the alloying degree increases to provide the requested capacity of 400 $mAhg^{-1}$, considering that some Sn particles become progressively inactive do to cracking failure. Obviously, this model requires future study to be effectively proposed to account for the voltage profile evolution observed in Figure 6.

To further evidence their practical relevance, the tin electrodes developed in this work have been tested as anode in a complete lithium ion cell using a high voltage, nickel manganese spinel, $LiNi_{0.5}Mn_{1.5}O_4$, as the cathode and a typical EC:DMC $LiPF_6$ solution as the electrolyte.

The steady-state electrochemical process of this cell is assumed to be:

$$xLiNi_{0.5}Mn_{1.5}O_4 + Sn \underset{\text{discharge}}{\overset{\text{charge}}{\leftrightarrows}} Li_xSn + Li_{(1-x)}Ni_{0.5}Mn_{1.5}O_4 \qquad (10)$$

Figure 7 shows the voltage profile of a Sn-5 (B) and of the $LiNi_{0.5}Mn_{1.5}O_4$ cathode (A) vs. specific capacity measured versus a Li foil electrode during the cell activation step.

Clearly, the specific capacity of the first cathode oxidation (160 $mAhg^{-1}$) is higher than the expected theoretical value (147.8 $mAhg^{-1}$) due to the electrolyte oxidation, especially at this low rate, and to initial spinel structure reorganization [11,12]. The Sn-5 anode is activated by discharging it at full capacity.

After this activation step the complete Sn-5 / EC-DMC 1:1 LiPF6 1M / $LiNi_{0.5}Mn_{1.5}O_4$ battery is assembled and tested. Since the battery is cathode limited at 0.2 mAh (147.8 $mAhg^{-1}$ vs. cathode active mass), the corresponding cycling capacity of the Sn anode is 400 $mAhg^{-1}$, namely the limited value under which the electrode is expected to perform with good cycle life, se Fig. 5B.

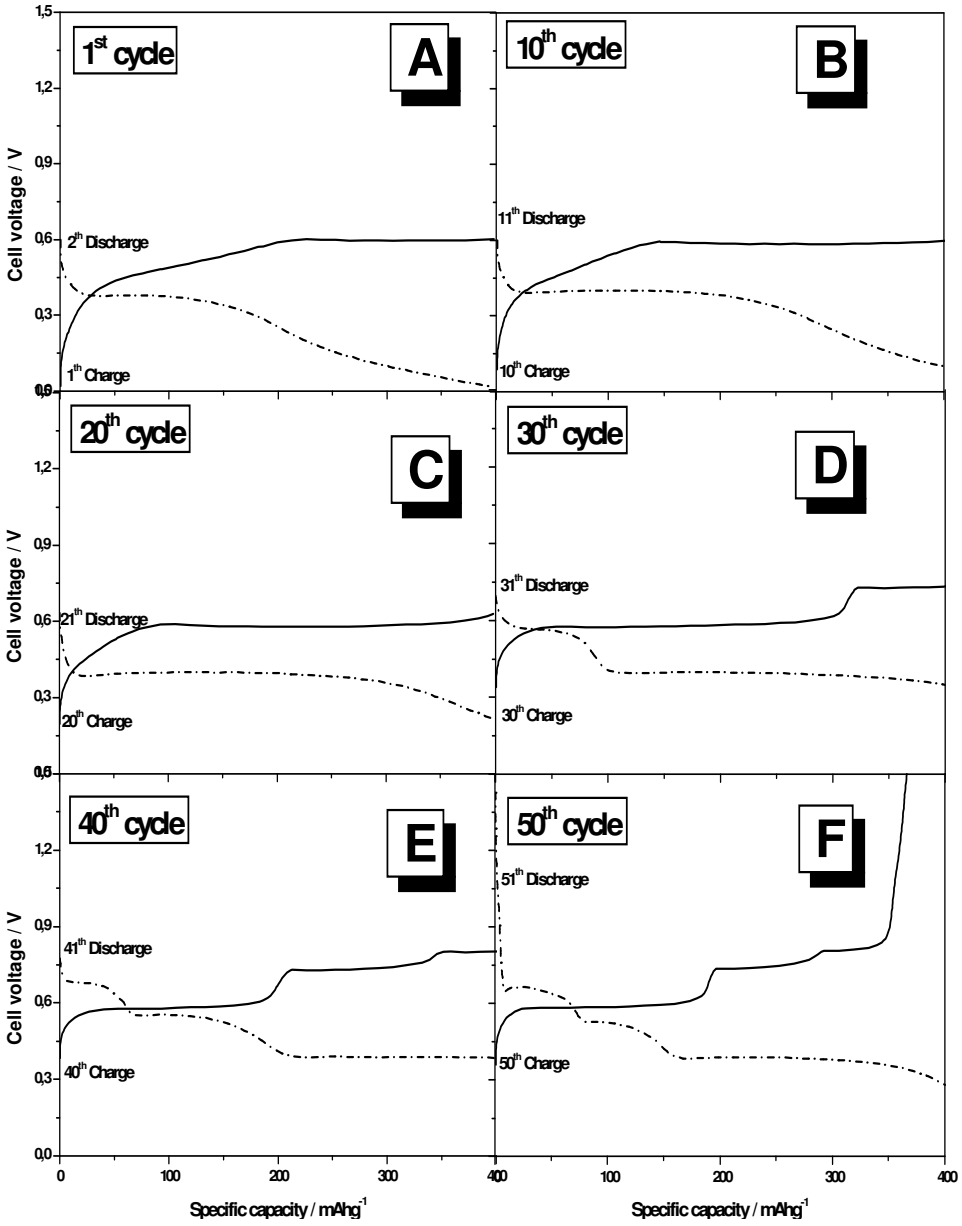

Figure 6. Cell voltage vs. specific capacity profiles for 1st (A)and 10th (B), 20th (C), 30th (D), 40th (E) and 50th (F) cycle for limited capacity test using sample Sn-5 as cathode in a lithium cell, EC:DMC 1:1 $LiPF_6$ electrolyte. Charge-discharge current density: 1$Acm^{-2}g^{-1}$, about 0.8C rate. Room temperature. For samples' identification see Table 1.

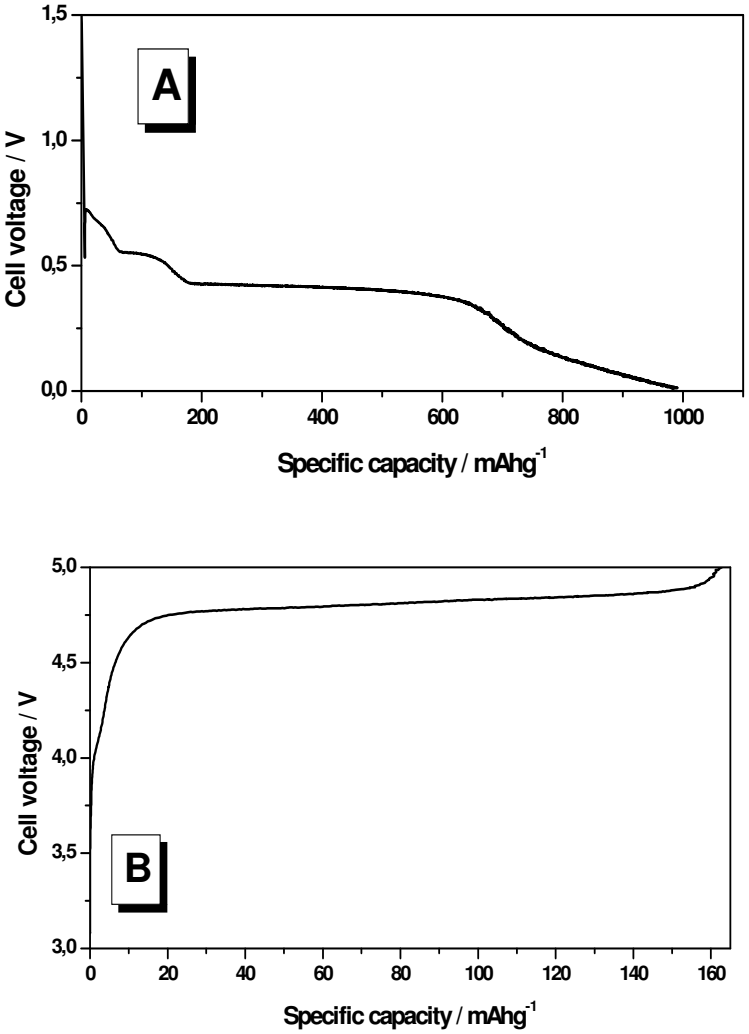

Figure 7. Discharge voltage of Sn (A) and charge voltage $LiNi_{0.5}Mn_{1.5}O_4$ (B) vs. specific capacity for activation versus 3rd Li foil electrode of a Sn-5 / EC:DMC 1:1 $LiPF_6$ / $LiNi_{0.5}Mn_{1.5}O_4$ lithium ion cell. Charge-discharge current density: 0.2 $Acm^{-2}g^{-1}$ vs. $LiNi_{0.5}Mn_{1.5}O_4$, about 1C rate. Room temperature. For samples' identification see Table 1

This is confirmed by Fig. 8A which reports the voltage profile of some typical charge-discharge cycles and by Fig. 8B which illustrates the capacity (referred to the cathode and the anode active mass) delivered upon cycling. The cell operates around 4.5 V with a good charge-discharge efficiency (99 %) and with a high reversible capacity, i.e. around 135 $mAhg^{-1}$ (about 92 % of theoretical) at relatively high 1C rate (147,8 mAg^{-1}) assuring high specific energy density (approaching 608 $mWhg^{-1}$) and high specific power (approaching 660 mWg^{-1}). As expected, the capacity profile reproduces that observed in the controlled capacity test of sample Sn-5, compare Figure 5B.

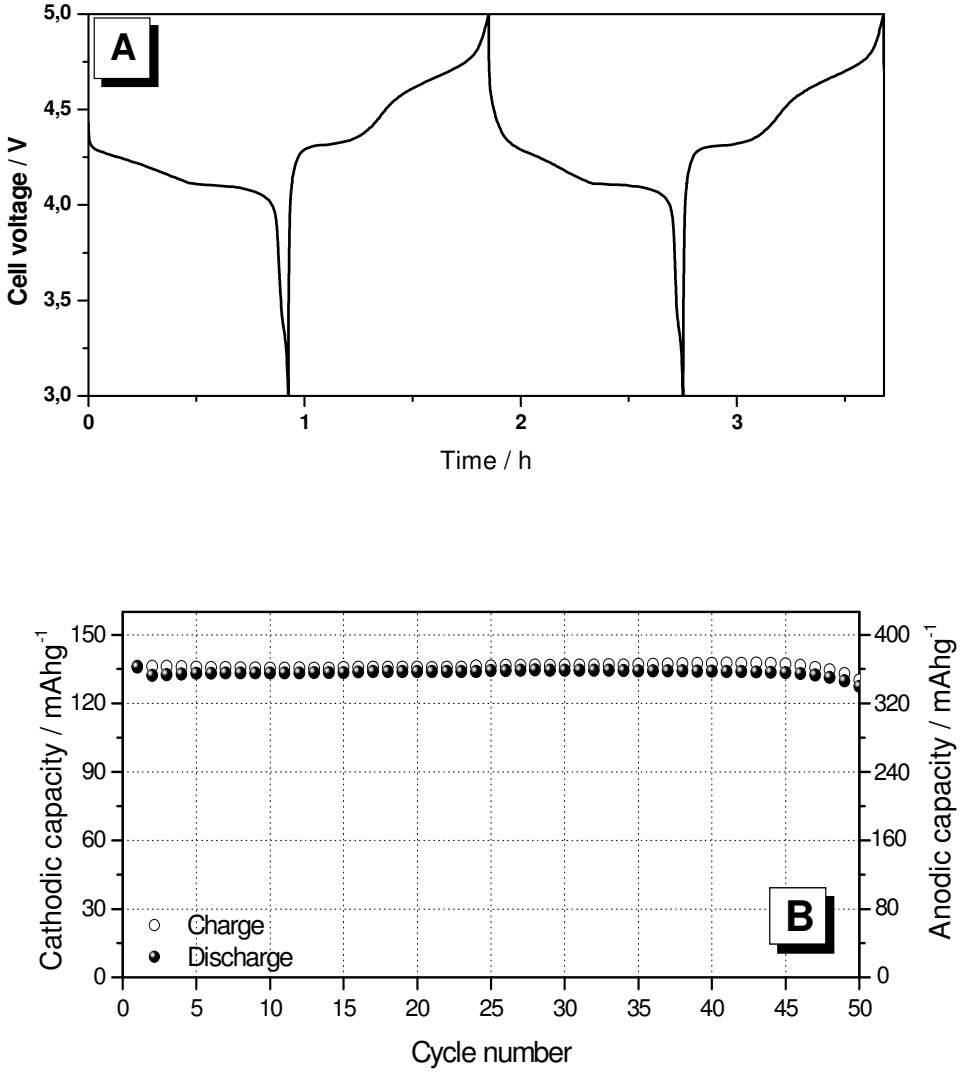

Figure 8. Voltage-time profiles of typical charge-discharge cycles (A) and capacity delivered upon cycling of a Sn-5 /. EC:DMC 1:1 $LiPF_6$ / $LiNi_{0.5}Mn_{1.5}O_4$ lithium ion cell. Charge-discharge current density: 0.2 $Acm^{-2}g^{-1}$ vs. $LiNi_{0.5}Mn_{1.5}O_4$, about 1C rate. Room temperature. For samples' identification see Table 1

Figure 9 shows cell voltage vs. specific capacity profiles for 1st (A), 10th (B), 20th (C), 30th (D), 40th (E) and 50th (F) cycle for this Sn-5 / EC:DMC 1:1 $LiPF_6$ / $LiNi_{0.5}Mn_{1.5}O_4$ lithium ion battery. The good, reproducible behaviour, already stressed in figure 8, is here confirmed, this finally marking, this new type of lithium ion battery of interest for specific applications where high rate, low cost and environmental compatibility are the priority requisites.

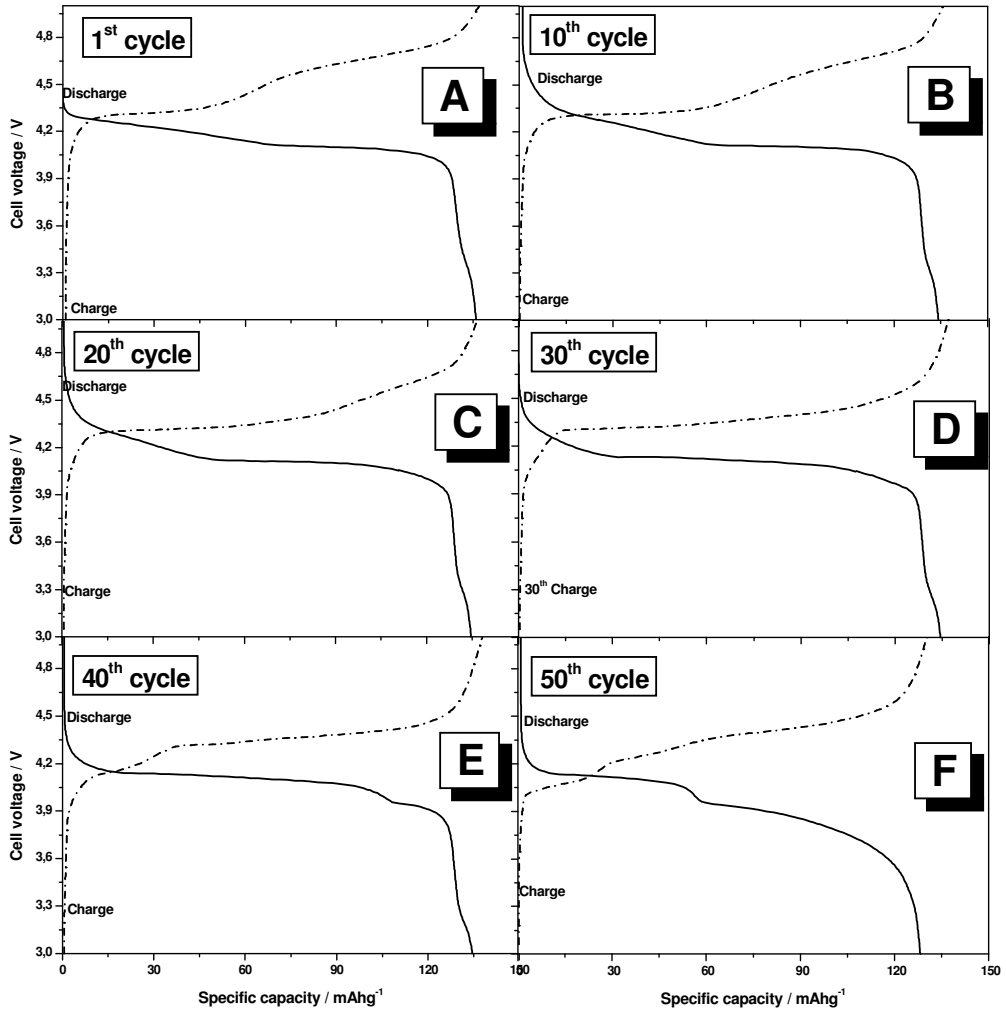

Figure 9. Cell voltage vs. specific capacity profiles for 1st (A)and 10th (B), 20th (C), 30th (D), 40th (E) and 50th (F) cycle for of a Sn-5 /. EC:DMC 1:1 $LiPF_6$ / $LiNi_{0.5}Mn_{1.5}O_4$ lithium ion cell. Charge-discharge current density: 0.2 $Acm^{-2}g^{-1}$ vs. $LiNi_{0.5}Mn_{1.5}O_4$, about 1C rate. Room temperature. For samples' identification see Table 1

4. CONCLUSIONS

The results reported in this work confirm that the electroplating is a very promising synthesis tool for monitoring the morphological characteristics of lithium ion electrodes such as tin electrodes. Moreover, here we demonstrate that a proper cycling condition is a crucial parameter for optimizing the cycle life of these Sn-based electrodes.

Further work is certainly necessary to refine the limited capacity approach here described. However, the results reported in this work, even it preliminary, are quite promising to demonstrate the validity of this approach, as confirmed by the good response of the Sn electrodes as anodes in a new type of a lithium ion battery.

Although having a relatively short life, this battery is of practical interest due to its low cost, high specific energy density, high power and high rate performance. In addition, it is expected that by optimizing the electrode morphology and capacity regime, the cycle life and the power capability can be further improved. This attempt is in progress in our laboratory and the result will be reported in future paper.

ACKNOWLEDGEMENT

This work has been carried out with the financial support of the European Network of Excellence ALISTORE and of the Italian Ministry of University and Research under a PRIN 2005 project.

References.

1. A. Finke, P. Poizot, C. Guéry, and J-M. Tarascon, *J. Electrochem. Soc.,* 152 ,12 (2005) 2364
2. Y. S. Fung, and D. R. Zhu, *J. Electrochem. Soc.*, 149,3 (2002) 319
3. S. D. Beattie and J. R. Dahn, *J. Electrochem. Soc.*, 150,7 (2003) 894
4. Il-seok Kim, G. E. Blomgren, and P. N. Kumta, *Electrochem. & Solid-State Letters*, 7,3 (2004)
5. Ou Mao, R. A. Dunlap, and J. R. Dahn, *J. Electrochem. Soc.,* 146,2 (1999) 405
6. I. Amadei, S. Panero, B. Scrosati, G. Cocco, L. Schiffini, *J. Power Sources*, 143 (2005) 227
7. H. Mukaibo, T. Sumi, T. Yokoshima, T. Momma, T. Osaka, *Electrochem. & Solid-State Lett* , 6 (2003) 218
8. J.Hassoun, S.Panero, B.Scrosati, *J. Power Sources*, (2006), in press
9. P. Reale, S. Panero, and B. Scrosati, *J. Electrochem. Soc.,* 152 ,10 (2005) 1949
10. C.J. Wen, R.A. Huggins, *J. Electrochem. Soc.*, 128 (1981) 1181
11. A. Caballero, L. Hernán, J. Morales and M. Angulo, *Electrochem. & Solid-State Lett.* 152, 1 (2005) 6
12. J.C. Arrebola, A. Caballero L. Hernán and J. Morales, *Electrochem. & Solid-State Lett.* 152, 3 (2005) 641